

ON SCALING PROPERTIES OF THIRD-ORDER RESONANCE  
CROSSING  
IN PARTICLE ACCELERATORS

S.Y. Lee

*Indiana University, Bloomington, IN 47405*

K.Y. Ng

*Fermilab, Batavia, IL 60510*

*Abstract*

The effects of charged particle beams crossing a third-order resonance in an accelerator are studied. A 20% emittance growth or 2.5% of trap-fraction can be used to define the critical or tolerable resonance strength, which is found to follow simple scaling laws vs tune-ramp rate and initial emittance. One scaling law can be derived by solving Hamilton's equations of motion in a perturbative approach. Such scaling laws can be used to evaluate the performance of high power accelerators, such as fixed-field alternating-gradient accelerators (FFAGs) and cyclotrons [6].

Submitted to  
52<sup>nd</sup> ICFA Advanced Beam Dynamics Workshop on  
High-Intensity and High-Brightness Hadron Beams (HB2012)  
Beijing, China  
September 17–21, 2012

# On scaling properties of third-order resonance crossing in particle accelerators\*

S.Y. Lee, Indiana University, Bloomington, IN 47405, US  
K.Y. Ng, Fermilab, Batavia, IL 60510, US

## Abstract

The effects of charged particle beams crossing a third-order resonance in an accelerator are studied. A 20% emittance growth or 2.5% of trap-fraction can be used to define the critical or tolerable resonance strength, which is found to follow simple scaling laws vs tune-ramp rate and initial emittance. One scaling law can be derived by solving Hamilton's equations of motion in a perturbative approach. Such scaling laws can be used to evaluate the performance of high power accelerators, such as fixed-field alternating-gradient accelerators (FFAGs) and cyclotrons [6].

## INTRODUCTION

The third-order resonance plays a dominant role in dynamic aperture and may also limit accelerator performance [1, 2, 3, 4]. In particular, the betatron tunes of *non-scaling* FFAGs are designed to ramp through many resonances during the acceleration process. We study here the fractional emittance growth (FEG) and particle trap-fraction after crossing the third-order resonance. Our aim is to derive scaling laws for a tolerable resonance strength. The results will be compared with multi-particle tracking [5]. The model ring used for tracking resembles the Fermilab Booster, which is of circumference 474 m, composed of 24 FODO cells with 24-fold supersymmetry. The betatron functions at the quadrupoles are  $\beta_x^F = 40$  m,  $\beta_z^F = 8.3$  m,  $\beta_x^D = 6.3$  m,  $\beta_z^D = 21.4$  m. A sextupole and an octupole are placed at one of the D-quads to generate the third-order resonance strength  $G$  and the horizontal detuning  $\alpha$ . The beam kinetic energy is kept at 1 GeV. The horizontal tune is ramped from  $\nu = 6.40$  to 6.28 crossing the  $3\nu = \ell$  resonance, while the vertical tune is fixed at 6.45. In general, 5000 macroparticles are used, initially in a 6- $\sigma$ -truncated Gaussian distribution of rms emittance  $\epsilon_i$ .

## HAMILTONIAN AND FIXED POINTS

We start from the Hamiltonian [7]

$$H = \delta I + \frac{1}{2}\alpha I^2 + GI^{3/2} \cos 3\psi \quad (1)$$

in the horizontal phase space, describing the action  $I$  and angle  $\psi$  of a particle in the rotational frame of a third-order resonance, where  $G$  is the absolute value of the resonance strength and  $\delta = \nu - \ell/3$  is the proximity of the horizontal betatron tune  $\nu$  to the resonance at  $3\nu = \ell$ . The Hamilton's equations of motion are

$$\dot{I} = 3GI^{3/2} \sin 3\psi, \quad \dot{\psi} = \delta + \alpha I + \frac{3}{2}GI^{1/2} \cos 3\psi. \quad (2)$$

\*Work supported by the US DOE under contracts DE-FG02-92ER40747, DE-AC02-76CH030000, and the NSF under contract NSF PHY-0852368.

When  $\alpha > 0$ , unstable fixed points (UFPs) are given by

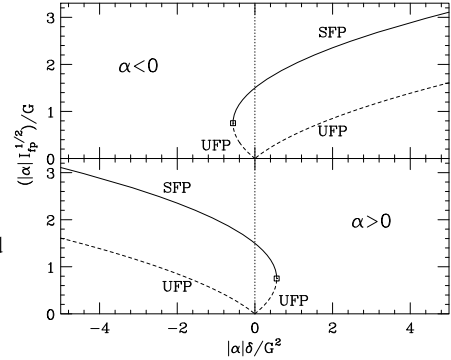
$$\frac{\alpha I_{\text{ufp}}^{1/2}}{G} = \mp \frac{3}{4} \pm \frac{3}{4} \sqrt{1 - \frac{16\alpha\delta}{9G^2}}, \quad \begin{cases} \delta < 0, \\ 0 \leq \delta \leq 9G^2/16\alpha, \end{cases}$$

with  $\psi_{\text{ufp}} = 0, \pm 2\pi/3$  changing to  $\pi, \pm\pi/3$  as  $\delta$  changing from negative to positive. The stable fixed points (SFPs) are given by

$$\frac{\alpha I_{\text{sfp}}^{1/2}}{G} = +\frac{3}{4} + \frac{3}{4} \sqrt{1 - \frac{16\alpha\delta}{9G^2}}, \quad \delta \leq 9G^2/16\alpha, \quad (3)$$

with  $\psi_{\text{sfp}} = \pi, \pm\pi/3$ . These are shown in Fig. 1. The total area of the three resonance islands is approximately  $\frac{16}{\pi} G^{1/2} |\delta|^{3/4} |\alpha|^{-5/4}$ .

Figure 1: Fixed points  $|\alpha|I_{\text{fp}}^{1/2}/G$  vs  $|\alpha|\delta/G^2$  for  $\alpha < 0$  (top) and  $\alpha > 0$  (bottom). Bifurcation occurs at  $\delta_{\text{bif}} = 9G^2/(16|\alpha|)$  and is marked by a rectangle.



## RING BEAM AND ADIABATIC RAMPING

Without loss of generality, we consider only downward ramping of the horizontal tune. As shown in Fig. 1, the resonance islands move outward with increasing size at positive detuning, trapping particles. This is demonstrated by simulating a ring of particles in Fig. 2. It is apparent that the emittance increases without limit. As a result, the resonance crossing effects are characterized by the fraction of particles trapped inside the islands.

On the other hand, with negative detuning, the resonance islands move inward and no particles can be trapped.

Figure 2: (Color) Evolution of a ring of particle showing some captured into resonance islands. Tune-ramp rate is  $d\nu/dn = -2 \times 10^{-5}$  at detuning  $\alpha = 500 (\pi\text{m})^{-1}$  and resonance strength  $G = 0.2 (\pi\text{m})^{-1/2}$ .

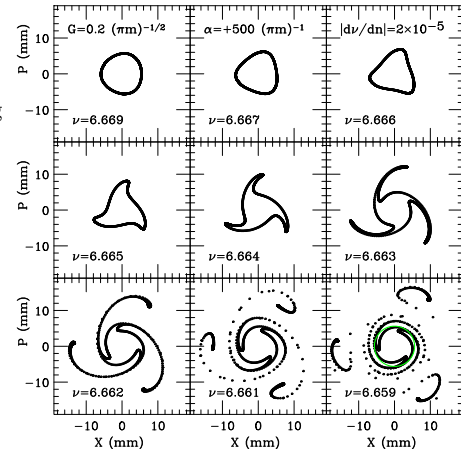
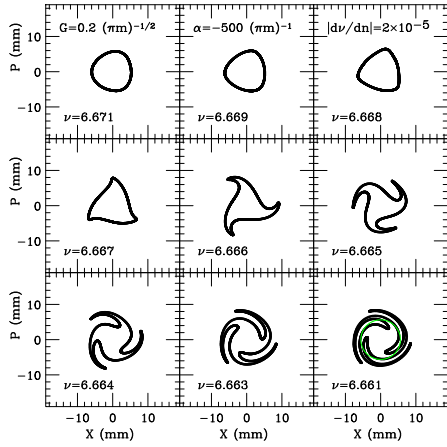
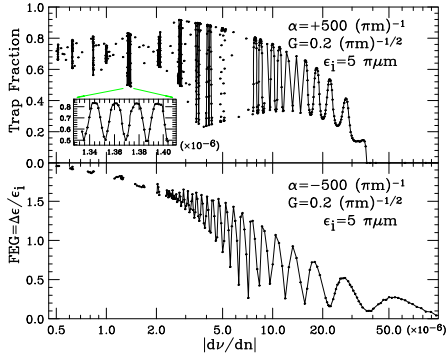


Figure 3:  
(Color) Evolution of a ring of particles showing emittance increasing without captured into resonance islands with the same parameters as in Fig. 2, but with detuning parameter  $\alpha = -500 (\pi\text{m})^{-1}$ .



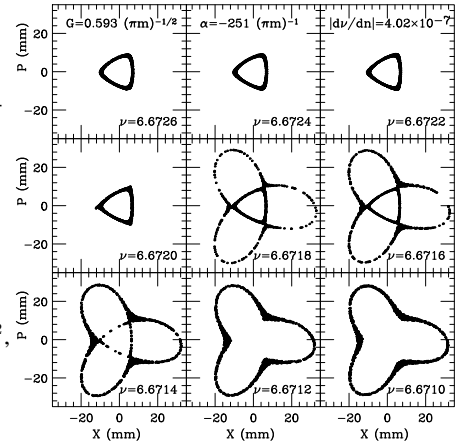
However, the emittance will increase because particles will stream along island separatrices. The characterization here is the fractional emittance growth,  $\text{FEG} = \Delta\epsilon_i/\epsilon_i$ , where  $\epsilon_i$  is the initial rms emittance of the beam. This is demonstrated by simulating a ring of particles in Fig. 3. Figure 4 shows the FEG and trap-fraction exhibiting oscillations, which die down at adiabatic tune-ramping rates,  $|dv/dn| \lesssim 5 \times 10^{-7}$ . The oscillatory structure reflects the exact timing when the particles encounter the fixed points. If particles accumulate near the UFPs, the FEG will be large. If particles accumulate near SFPs, the FEG will be small but the trap-fraction will be large. Since the starting conditions are the same for all simulations, the timing dependency is translated to the tune-ramp rate instead.

Figure 4:  
(Color) Trap-fraction (top) and FEG (bottom) vs tune-ramp rate for  $\alpha > 0$  and  $< 0$ . Wide oscillations are observed except at adiabatic tune-ramp rates.



We now examine the physics of the adiabatic FEG limit when  $\alpha < 0$ . As the resonance moving inward reaches the ellipse of particles, Fig. 5 shows that the phase space is adiabatically deformed to the inner separatrix of the islands, and as the resonance moves away, particle will be distributed along the outer orbit of the separatrices. The FEG is the ratio of the island-area divided by the initial phase-space area, which is equal to the inner area bounded by the separatrices shown in the top four plots of Fig. 5. As the resonance collapses after bifurcation, the phase-space ellipse follows the Hamiltonian torus and the phase-space area does not change. We calculate the island areas of the resonance Hamiltonian at the instant that the inner stable area is equal to the initial phase-space ellipse, which is depicted as green dashes in Fig. 6. It fits the simulation data fairly well, and reveals a scaling law  $\text{FEG} \approx 7.3 S_{\text{ad}}$ , where the adiabatic-ramping scaling parameter is  $S_{\text{ad}} =$

Figure 5:  
(Color) Evolution of a ring of particles at adiabatic tune ramp rate  $dv/dn = -4 \times 10^{-7}$ , detuning  $\alpha = -251 (\pi\text{m})^{-1}$  and resonance strength  $G = 0.593 (\pi\text{m})^{-1/2}$  showing emittance increase up to separatrix.

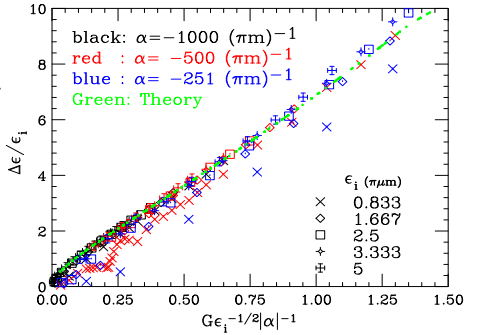


$G/(\epsilon_i^{1/2}|\alpha|)$ . For a beam of initial distribution  $\rho(I)$ , the FEG after crossing the third-order resonance is

$$\text{FEG} = 7.3 \int \frac{G\sqrt{I}}{\epsilon_i|\alpha|} \rho(I) dI = 7.3 \Gamma\left(\frac{3}{2}\right) \frac{G}{|\alpha|\epsilon_i^{1/2}}, \quad (4)$$

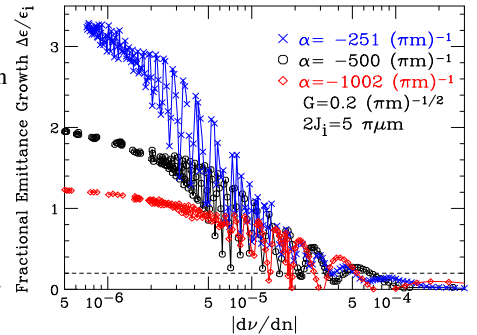
where a Gaussian bunch of initial rms emittance  $\epsilon_i$  is assumed in the last step and  $\Gamma(\frac{3}{2})$  is the Gamma function.

Figure 6:  
(Color) Simulation data of adiabatic tune-ramp rate at negative detuning obey a scaling law with scaling parameter  $S_{\text{ad}} = G/(\sqrt{\epsilon_i}|\alpha|)$ .



For FFAGs, the adiabatic FEG is too large to be acceptable in practice. The tune-ramp rate usually depends on energy gain per turn, and one often tries to ramp through the resonances as fast as possible. The typical tune-ramp rate is about  $10^{-3} \sim 10^{-5}$  per revolution. Figure 7 shows that the FEG becomes detuning independent when the tune-ramp rate is higher than  $\sim 10^{-5}$ .

Figure 7:  
(Color) Dependence of FEG on detuning at adiabatic tune-ramp rates disappears mostly at higher tune-ramp rates  $|dv/dn| \gtrsim 10^{-5}$ .



## NON-ADIABATIC RAMPING

### Scaling Law for negative detuning

To understand how emittance increases on passing through the third-order resonance at negative detuning, we investigate the action change of a particle near the outer-most of the beam. In particular, we are interested in the

particle that collides with an UFP at turn  $n_{\text{ufp}}$ , when  $\dot{I} = 0$  and  $\dot{\psi} = 0$ . To study the particle motion near the UFP, we Taylor expand its action-angle about the UFP. Since the betatron tune is ramping,  $\dot{\psi} = \delta = \frac{1}{2\pi} \frac{d\nu}{dn}$ . At turn  $n$ ,

$$\Delta I \approx 6\pi^2 G I_{\text{ufp}}^{3/2} \cos 3\psi_{\text{ufp}} \frac{d\nu}{dn} (\Delta n)^3, \quad \Delta\psi \approx \pi \frac{d\nu}{dn} (\Delta n)^2, \quad (5)$$

where  $\Delta I = I_f - I_{\text{ufp}}$  with  $I_f$  the final action, and  $\Delta n = n - n_{\text{ufp}}$ . At negative detuning, when the betatron tune is ramped downward, the UFP moves inwards as the proximity  $\delta$  decreases from a positive value to zero. Equation (3) indicates that  $\psi_{\text{ufp}} = \pi, \pm\pi/3$ . Thus the action of the particle increases after passing the UFP. The motion of the particle before colliding with the UFP is the reciprocal of what happens after colliding with the UFP. Therefore

$$I_{\text{ufp}} \approx \frac{1}{2} (I_i + I_f) = I_i \left( 1 + \frac{\Delta I}{2I_i} \right), \quad (6)$$

where  $I_i/I_f$  is the initial/final action of the particle. We next make the identification of the particle's action at the outer-edge of the beam with the beam emittance; i.e.,  $I_i = 3\epsilon_i$  and  $I_f = 3\epsilon_f$ , with  $\epsilon_f$  being the final rms emittance of the beam, to arrive at a relation between the emittance growth  $\Delta\epsilon/\epsilon_i$  and the change in particle phase  $\Delta\psi$ :

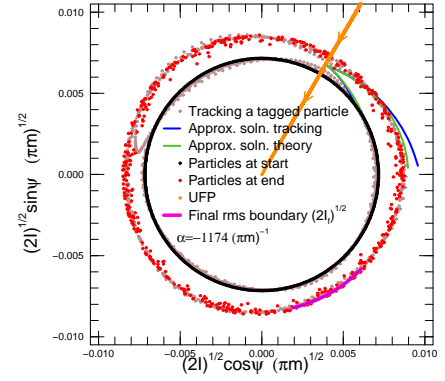
$$\frac{\Delta\epsilon}{\epsilon_i} = \frac{12\sqrt{3}\pi G \epsilon_i^{1/2} (\Delta\psi)^{3/2}}{\sqrt{|d\nu/dn|}} \left( 1 + \frac{\Delta\epsilon}{2\epsilon_i} \right)^{3/2}. \quad (7)$$

It is evident that the relation is independent of the detuning  $\alpha$  and is dependent on only one scale parameter

$$S = G \sqrt{\frac{\epsilon_i}{|d\nu/dn|}}. \quad (8)$$

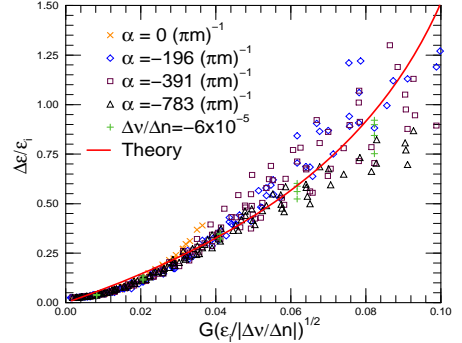
A simulation was performed to illustrate the emittance growth by tracking the Hamiltonian of Eq. (1) using a symplectic integrator. The outer edge of a Gaussian bunch of rms emittance  $\epsilon_i = 8.54 \mu\text{m}$  has initial action  $I_i = 3\epsilon_i = 25.62 \mu\text{m}$ , where a ring of 500 macroparticles are placed. The resonance strength is  $G = 0.1483 (\pi\text{m})^{-1/2}$ , the detuning is  $\alpha = -937.5 (\pi\text{m})^{-1}$ , and the tune-ramp rate is  $d\nu/dn = -6 \times 10^{-5}$ . We start the tracking at a time when the UFP has an action  $I_{\text{ufp}} = 4I_i$ , with initial proximity parameter  $\delta_i = -\alpha I_{\text{ufp}} - \frac{3}{2} G I_{\text{ufp}}^{1/2} \cos 3\psi_{\text{ufp}} = 0.123$  and the proximity at bifurcation  $\delta_{\text{bif}} = 9G^2/(16|\alpha|) = 1.05 \times 10^{-5}$ . It will take  $(\delta_i + \delta_{\text{bif}})/|d\nu/dn| = 2043$  turns to ramp the proximity to pass bifurcation. The results are shown in Fig. 8. We also show the trajectory of one tagged particle initially at  $\psi = 0$  in brown. After a near encounter with an UFP at  $\psi = \pi$ , the particle reverses direction with an increase in action. The motion of the action of a hypothetical particle colliding exactly with the UFP at  $\psi = \pi/3$  is depicted in green according to the Taylor expansion in Eq. (5), which nearly overlaps the tracked trajectory of this hypothetical particle shown in blue. The trajectory of the UFP at  $\psi = \pi/3$  moving inward is shown in orange. The change in the particle's phase during the resonance crossing is  $\Delta\psi \approx \pi/10$ , and remains roughly the same when simulation parameters are varied. This simulation verifies the process of emittance increase after encountering an UFP.

Figure 8: (Color) Tracking a ring of 500 particles across a third-order resonance. The trajectory of the tagged particle (brown) shows a change in phase  $\Delta\psi \approx \pi/10$ .



To verify the scaling law derived in Eq. (7), we compile and plot in Fig. 9 a large amount of tracking results of the model ring (not the Hamiltonian in  $I$  and  $\psi$ ) over a wide area of the parameter space: detuning from  $\alpha = 0$  to  $-800 (\pi\text{m})^{-1}$ , resonance strength from  $G = 0.02$  to  $0.8 (\pi\text{m})^{-1/2}$ , initial rms emittance from  $\epsilon_i = 0.925$  to  $9.25 \mu\text{m}$ , and tune-ramp rate from  $|d\nu/dn| = 10^{-5}$  to  $10^{-2}$ . On top is plotted in red the scaling law derived in Eq. (7) with  $\Delta\psi = \pi/10$  substituted. The verification of the scaling law is remarkable. The widespread of simulation data at larger scaling parameter  $S$  has a similar explanation as the large-amplitude oscillations in Fig. 4. The independence of FEG on detuning parameter is shown in the left plot of Fig. 10 for four different values of detunings.

Figure 9: (Color) FEG from simulation data vs scaling parameter  $S = G \sqrt{\epsilon_i/|d\nu/dn|}$ , fall on the derived scaling law of Eq. (7) (red) very well.



Although Eq. (5) appears to be an expansion in  $\Delta\theta = 2\pi\Delta n$ , which is a large number, however, when the expansion is continued to a few more terms, we find that the perturbation is actually a power series expansion in  $[G I_{\text{ufp}}^{1/2} 2\pi\Delta n]^2 \approx 12\pi S^2 \Delta\psi$ , which turns out to be  $\sim 0.12$  when  $S = 0.1$  and  $\Delta\psi = \pi/10$  are substituted. For this reason, Eq. (5) is not applicable to adiabatic tune ramping, where  $S$  might be large. The scaling law for adiabatic tune ramping in Eq. (4) was obtained from solving the Hamiltonian exactly in a non-perturbative manner.

### Tolerable resonance strength

Figure 10 shows on the right the FEG vs resonance strength from simulations for various tune-ramp rates, but at fixed initial rms emittance  $\epsilon_i = 4.62 \mu\text{m}$  and detuning  $\alpha = -391 (\pi\text{m})^{-1}$ . Here we set 20% as the tolerable emittance increase for crossing the third-order resonance. Then the corresponding critical or tolerable resonance strength  $[G]_{\text{FEG}=0.2}$  can be read off readily for each tune-ramp rate.

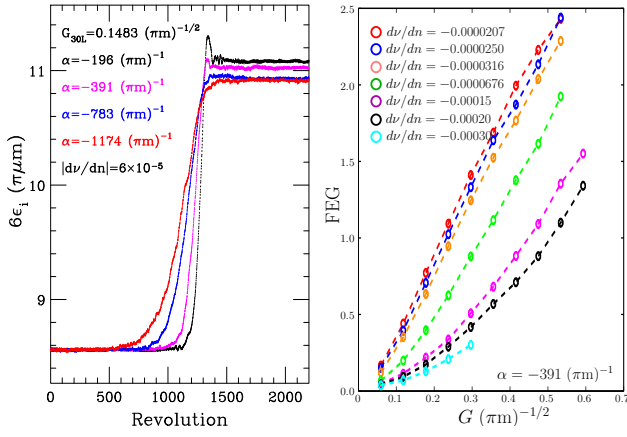


Figure 10: (Color) Left: Emittance growth when passing through a third-order resonance at tune-ramp rate  $|\dot{\nu}/dn| = 6 \times 10^{-5}$  and resonance strength  $G = 0.1483 (\pi \text{ mm})^{-1/2}$  for various detuning parameters. Right: FEG vs resonance strength  $G$  for a wide range of tune-ramp rates at initial rms emittance  $\epsilon_i = 4.62 \pi \mu\text{m}$  and detuning  $\alpha = -391 (\pi \text{ mm})^{-1}$ .

Similarly,  $[G]_{\text{FEG}=0.2}$  can be extracted from simulations with other detunings and initial rms emittances. Finally, we plot  $[G]_{\text{FEG}=0.2} \epsilon_i^{1/2}$  vs  $|\dot{\nu}/dn|$  in Fig. 11. All data fall roughly on the scaling law

$$[G]_{\text{FEG}=0.2} = 0.027 \epsilon_i^{-1/2} \left| \frac{d\nu}{dn} \right|^{1/2}. \quad (9)$$

Actually, the above can be derived directly from the scaling law derived in Eq. (7) with  $\Delta\psi = \pi/10$  or Fig. 9. The FEG = 20% corresponds to  $S = 0.027$ , and Eq. (9) follows. We note that the quantity  $G \epsilon_i^{1/2}$  is dimensionless and constitutes a scaling parameter at constant tune-ramp rate. For this reason, it is sometimes called the *effective* resonance strength.

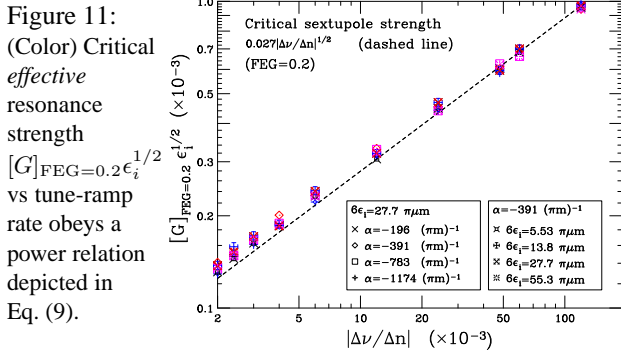


Figure 11: (Color) Critical effective resonance strength  $[G]_{\text{FEG}=0.2} \epsilon_i^{1/2}$  vs tune-ramp rate obeys a power relation depicted in Eq. (9).

## PARTICLE TRAPPING IN RESONANCE ISLANDS WHEN DETUNING $\alpha > 0$

Since particles will be trapped in islands when the detuning is positive and the tune is ramped downward, the trap-fraction is a more useful characterization of the resonance-crossing effects. However, it is more practical to define the trapped effect as  $f_{\text{trap}} = N_{I>I_{i,\text{max}}} / N_{\text{total}}$ , where  $N_{\text{total}}$  is the total number of particles in the beam and  $N_{I>I_{i,\text{max}}}$  is the number of particles with action  $I$  larger than that of

initial maximum after passing through the resonance, independent of whether they are trapped inside the resonance islands or they fall outside the islands while moving along the separatrices. Although this definition may differ from the trap efficiency employed in Ref. [2, 3], nevertheless, it should make comparison with experimental measurements more appropriate, where scraping is often used to remove large-amplitude particles.

This definition of trap-fraction has another merit that it can also be used to characterize resonance crossing effects even when the detuning is negative and there is no trapping by islands. Thus there is a correlation between FEG and  $f_{\text{trap}}$  at negative detuning, which is evident in the left plot of Fig. 12, where the critical or tolerable resonance strength  $[G]_{\text{FEG}=0.2}$  for an emittance increase of 20% in resonance crossing at negative detuning is equivalent to the critical or tolerable resonance strength  $[G]_{f_{\text{trap}}=2.5\%}$ , when 2.5% of particles are being excited to have actions larger than the initial maximum action of the beam.

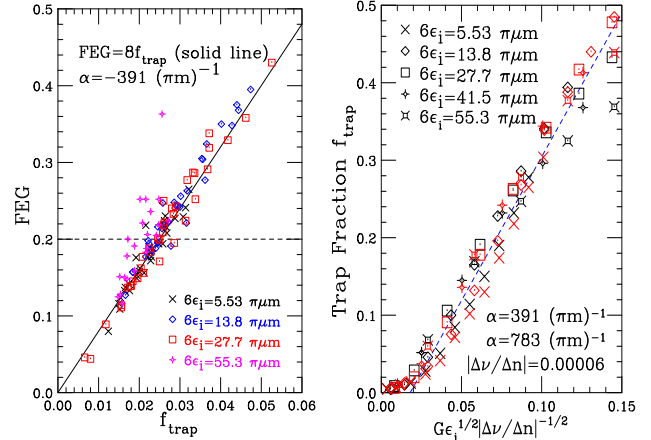


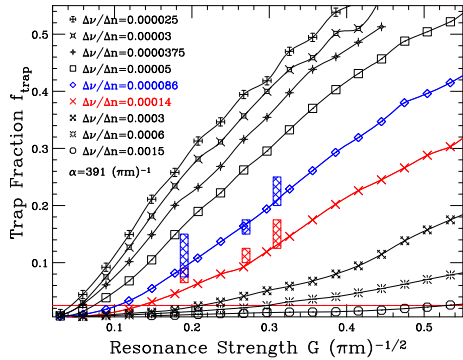
Figure 12: (Color) Left: Correlation between FEG and  $f_{\text{trap}}$  for  $\alpha < 0$  for beams with different emittances, resonance strengths and tune-ramp rates. Right: Trap-fraction vs scaling parameter  $S$  of Eq. (8) for a wide range of initial emittances, two detuning parameters, and a fixed tune-ramp rate  $\dot{\nu}/dn = -6 \times 10^{-5}$ .

Figure 13 shows the trap-fractions calculated for different tune-ramp rates with detuning parameter  $\alpha = 391 (\pi \text{ mm})^{-1}$ . Experimental data from Ref. [3] are also shown with blue and red boxes. They appear to agree reasonably well with our simulation results at tune-ramp rates  $-8.6 \times 10^{-5}$  and  $-1.4 \times 10^{-4}$ .

Similar to the scaling property shown in the previous section, an *equivalent resonance strength* can be defined as  $G \epsilon_i^{1/2}$ , which is dimensionless. Including the square root of the tune-ramp rate, this becomes the scaling parameter defined  $S$  in Eq. (8). The right plot of Fig. 12 shows  $f_{\text{trap}}$  vs  $S$  for various initial emittances and detunings, but for a fixed ramping rate of  $\dot{\nu}/dn = -6 \times 10^{-5}$ . The plot reveals a rough scaling behavior for  $f_{\text{trap}}$ . However, when tracking results corresponding to more detunings and tune-ramp rates are added, the data are not so well clustered.

We next read off the critical or tolerable resonance strength  $[G]_{f_{\text{trap}}=2.5\%}$  that produces a 2.5% trap-fraction. The equivalent critical resonance strength is plotted against

Figure 13:  
(Color)  
Trap-fraction  
 $f_{\text{trap}}$  vs reso-  
nance strength  
 $G$  for an initial  
rms emittance  
 $\epsilon_i = 4.62 \mu\text{m}$   
with various  
ramping rates at  
detuning  $\alpha =$   
 $391 (\text{mm})^{-1}$ .  
Experimental data from Ref. [3] are shown with blue and red  
boxes at tune-ramp rates  $8.6 \times 10^{-5}$  and  $1.4 \times 10^{-4}$ .



tune-ramp rate in Fig. 14. The tracking data exhibit scaling behavior and fall between two power relations:

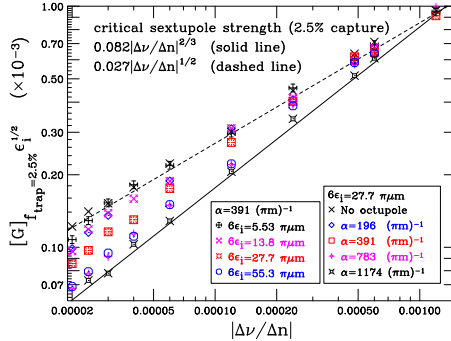
$$[G]_{f_{\text{trap}}=2.5\%} = 0.027\epsilon_i^{-1/2} \left| \frac{\Delta\nu}{\Delta n} \right|^{1/2}, \quad (10)$$

when the detuning is nearly zero (dashed line), and

$$[G]_{f_{\text{trap}}=2.5\%} = 0.082\epsilon_i^{-1/2} \left| \frac{\Delta\nu}{\Delta n} \right|^{2/3}, \quad (11)$$

when the detuning is as high as  $\alpha = 1174 (\text{mm})^{-1}$  (solid line). Notice that Eq. (10) is exactly the same as Eq. (9) at negative detuning, since  $[G]_{f_{\text{trap}}=2.5\%}$  is equivalent to  $[G]_{\text{FEG}=0.2}$ . We can draw the conclusion that the scaling curve at negative detuning for  $[G]_{\text{FEG}=0.2}$  is approximately the same as the scaling law for  $[G]_{f_{\text{trap}}=2.5\%}$  at positive detuning, at least in the small-positive-detuning regime.

Figure 14:  
(color) Equiva-  
lent critical reso-  
nance strength  
 $[G]_{f_{\text{trap}}=2.5\%}\epsilon_i^{1/2}$   
vs tune-ramp  
rate for various  
initial emit-  
tances, positive  
detunings, and  
tune-ramp rates.



*Comparison with the scaling law of Ref. [3]*

Aiba, *et al* define an adiabatic parameter in Eq. (27) of Ref. [3],

$$\eta_{\text{ad}} = \left( \frac{|\dot{\nu}/\dot{n}|}{3^{1/2}36|\alpha|G\epsilon_i^{3/2}} \right)^{2/3}, \quad (12)$$

where our notations have been used, and derive a trapping efficiency in their Eq. (33),

$$P_T = \frac{\pi}{2^{1/2}} \left( \frac{G}{3^{1/3}|\alpha|\epsilon_i^{1/2}} \right)^{1/2} \eta^{-1/4} e^{-\eta_{\text{ad}}}, \quad (13)$$

where  $\eta = \eta_{\text{ad}}$  or 1 according to  $\eta_{\text{ad}} \geq 1$ . Although their definition of trapping efficiency may be different from our  $f_{\text{trap}}$ , the scaling law should be universal. Equation (13), however, differs markedly from our scaling laws for the

FEG and  $f_{\text{trap}}$ , having different dependency on resonance strength  $G$ , initial rms emittance  $\epsilon_i$ , tune-ramp rate  $d\nu/dn$ , as well as detuning parameter  $\alpha$ . As an example, with  $G = 0.2 (\text{mm})^{-1/2}$ ,  $\epsilon_i = 10 \mu\text{m}$ ,  $|\alpha| = 100 (\text{mm})^{-1}$ , and  $|d\nu/dn| = 1 \times 10^{-5}$ ,  $\eta_{\text{ad}} = 0.19$  and Eq. (13) reduces to

$$P_T \approx \frac{\pi}{2^{1/2}} \left( \frac{G}{3^{1/3}|\alpha|\epsilon_i^{1/2}} \right)^{1/2}, \quad (14)$$

which is proportional to  $|\alpha|^{-1/2}$ . When  $\eta_{\text{ad}}$  increases to larger than one,  $P_T$  becomes proportional to  $|\alpha|^{-1/3}$ . In any case, increasing detuning will decrease trapping efficiency and therefore emittance growth; but this does not help much according to our scaling laws.

## CONCLUSIONS

We characterize the effects of a beam crossing the third-order resonance by the fractional emittance growth FEG and trap-fraction  $f_{\text{trap}}$ , and discover that a  $f_{\text{trap}} = 2.5\%$  at positive detuning is equivalent to a FEG = 0.2 at negative detuning.

From comparison with simulation results, the critical or tolerable resonance strengths,  $[G]_{\text{FEG}=0.2}$  and  $[G]_{f_{\text{trap}}=2.5\%}$ , are found to obey scaling laws, and the two are identical for small detunings.

The FEG at negative detunings can be derived from Hamilton's equations of motion in a perturbative approach, and is found to obey a scaling law with scaling parameter  $S = G\sqrt{\epsilon_i}/|d\nu/dn|$ .

Our method is also applicable to other resonances. For example, in crossing an octupole-driven resonance, the critical or tolerable resonance strength should scale like  $\sim \epsilon_i^{-1}|d\nu/dn|^{1/2}$  and should be nearly independent of the nonlinear detuning parameter. These results will be useful in the design of high power accelerators, in the estimate of the emittance growth in cyclotron, and as the requirement of slow-beam extraction using the third-order resonance [8].

## REFERENCES

- [1] P.A. Sturrock, *Annals of physics* **3**, 113-189 (1958).
- [2] A. Chao and M. Month, *Nucl. Instru. and Meth.* **121**, 129 (1974).
- [3] M. Aiba, et al, S. Machida, Y. Mori, and S. Ohnuma, *PRSTAB* **9**, 084001 (2006).
- [4] S.Y. Lee, et al, *Phys. Rev. Lett.* **67**, 3768 (1991).
- [5] S.Y. Lee, *Phys. Rev. Lett.* **97**, 104801 (2006); S.Y. Lee, G. Franchetti, I. Hofmann, F. Wang, and L. Yang, *New J. Phys.* **8**, 291 (2006); X. Pang, et al, *Proc. HB2008*, p. 118 (2008), <http://accelconf.web.cern.ch/AccelConf/HB2008/papers/wga21.pdf>
- [6] T.R. Edgecock, *Proc. Int. Part. Acc. Conf. 2010*, p. 3593 (2010), <http://accelconf.web.cern.ch/AccelConf/IPAC10/papers/thxmh01.pdf>
- [7] see e.g. S.Y. Lee, *Accelerator Physics*, 2nd edition (World Scientific, Singapore, 2004).
- [8] R. Capii and M. Giovannozzi, *PRSTAB*, **7**, 024001 (2004).